CHAPTER V
ELECTROMECHANICAL PROPERTES OF MULTI-WALLED CARBON NANOTUBE/GELATIN HYDROGEL COMPOSITES: EFFECTS OF ASPECT RATIOS, ELECTRIC FIELD, AND TEMPERATURE

5.1 Abstract

The effects of multi–walled carbon nanotube (MWNT) aspect ratio, electric field strength and temperature on the electromechanical properties of MWNT/gelatin hydrogel composites were investigated. The highest aspect ratio of MWNT provides the composites with the highest dynamic moduli under electric field. The MWNT/gelatin hydrogel composites of 0.01, 0.1, 0.5, 1 vol% and the pure gelatin hydrogel possess the storage modulus sensitivity values of 0.69, 1.23, 0.94, 0.81 and 0.47, respectively, at 800 V/mm. The results can be interpreted in terms of the enhanced polarizability between the carboxyl groups of gelatin under the presence of MWNT. The effect of temperature on the electromechanical properties of MWNT/gelatin hydrogel composites investigated between 30 °C and 90 °C shows three distinct regimes of temperature-dependent storage modulus behavior. In the deflection testing, the effects of electric field on the deflection distance and the dielectrophoresis force of the MWNT/gelatin hydrogel composites were also investigated. MWNT/gelatin hydrogel composites suspended in the silicone oil between electrodes, respond rapidly with a deflection toward the anode site, indicating the attractive force between anode and the polarized carboxyl group as the gelatin structure possesses negative charges.

Keywords: Electromechanical properties; Actuator; Biopolymer; Gelatin; Hydrogels; Multi-walled carbon nanotubes.

5.2 Introduction

Electroactive polymers (EAPs) have been continuously utilized and developed for several applications such as muscle–like actuator, complaint electrode, robotics and drug release. Hydrogel is a promising material structure for the development of EAPs since it possess a reversible response subject to external stimuli such as temperature (Okano *et al.*, 1990; Zareie *et al.*, 2000), pH (Park *et al.*, 1992), ionic strength (Kim *et al.*, 1999; Kim *et al.*, 2002), and electric fields (Kaewpirom and Boonsang, 2006; Kim *et al.*, 2002; Tungkavet *et al.*, 2012). Gelatin is a one type of hydrogels or EAPs; it is a biopolymeric–protein derived from animal collagen by the thermal and hydrolyzing processes with either acid or bases. It is stable as a film, a hydrogel, or a composite (Yang *et al.*, 1997). Because gelatin possesses non–immunogenicity, biodegradability, biocompatibility, bioactivity and commercial availability at relatively low cost, it has been widely used in the medical fields such as drug delivery, wound dressings, and artificial muscles (Nguyen and Lee, 2010). Usually, gelatin is produced by denaturing a naturally derived collagen in a solution through either an acidic or base process at high temperature in which the triple-helix structure is split to random coil structure. During the gel forming process at the temperature around 40 °C, the gelatin random chain in a warm aqueous solution undergoes a disorder–order transition into the coil–helix structure when cooled (Ross-Murphy, 1992). However, gelatin exhibits poor water resistance and low mechanical properties when compared with synthetic polymers, these limit its possible application as an EAP (Tungkavet *et al.*, 2012). Therefore gelatin needs to be reinforced either through chemical crosslinking or using some filler materials. Chemical crosslinking enhances thermal and mechanical properties through covalent bonds between the reactive side groups in gelatin molecules. However, this process presents the residual crosslinking agents that lead to toxic side effects. The use of multiwall carbon–nanotube (MWNT) as a reinforcement in gelatin has been studied by Li *et al.* (2003). They studied gelatin with MWNTs that can be embedded as an additive to enhance the mechanical properties of the gelatin hydrogel. Haider *et al.* (2007) investigated the swelling of MWNT/gelatin hydrogel composites. MWNT could maintain the stability of the composites without crosslinking agent due to the

hydrophobic effect of the MWNT. Carbon nanotubes (CNTs) are an attractive form of carbon, consisting of concentric cylinders of graphite layer to graphene cylinders. CNTs diameters are smaller than conventional carbon or glass fibers about 1000 times. Usually, nanotube aspect ratios are over 1000. The structural characteristics of CNTs are high aspect ratio, high surface area, and excellent mechanical, electrical and thermal properties. The combination of CNTs/polymer composites can be used to enhance their mechanical properties despite undergoing large deformations without damage (Bower *et al.*, 1999; Qian *et al.*, 2000). Schadler *et al.* (1998) studied the stress transfer under tension and compression in carbon nanotube epoxy composites; the compression modulus is higher than the tensile modulus, indicating the stress transfer in the composites. Wagner *et al.* (1998) investigated stress the transfer between MWNT and a fiber in the polymer composites which the MWNT stress transfer efficiency is larger than fiber–based composites. Therefore MWNTs are excellent-promising-reinforcing materials for biopolymers that have been developed to several applications such as biosensor (Guo *et al.*, 1998), and bio-electronic materials (Macdonald *et al.*, 2005).

The objective of our investigation is to determine the electromechanical properties of Multi–Walled Carbon Nanotube/Gelatin hydrogel composites containing an anionic surfactant (i.e., sodium dodecylsulfate) as candidate materials for actuator. The electrical properties, thermal properties, and electrorheological properties were investigated in terms of MWNTs concentration and aspect ratios, electric field strength, and temperature.

5.3 Experimental

5.3.1 Materials

Gelatin (Type B, bovine skin) and sodium dodecyl sulfate (SDS) were purchased from Sigma Aldrich (Singapore) and Loba Chemie (India), respectively. Various multi-walled carbon nanotubes (MWNTs), as purchased from Alphanano Technology Co., ltd., China, have specified diameters of 3–10, 10–20, 20–30, and 30–50 nm.

5.3.2 Preparation of MWNT/Gelatin Hydrogel Composites

Various concentrations of MWNT; 0.01, 0.1, 0.5, and 1 vol%, were dispersed in aqueous mediums filled with 1 vol% of SDS by a transonicator (Elma, D 7284). For the preparation of a gelatin solution, 10 vol% of gelatin was dissolved in distilled water (pH = 6.40) at 40 °C overnight by magnetic stirring. Then, two solutions were well–mixed at 40 °C, and poured into a petri dish to obtain the MWNT/Gelatin hydrogel composites. The hydrogel composites were allowed to set as a sheet at 25 °C. The thickness of hydrogel composites was about 1.64 mm.

5.3.3 Characterization and Testing of MWNT/Gelatin Hydrogel Composites

True density of each multi-walled carbon nanotubes (MWNT) was measured by a gas pycnometer (Thermo Nicolet, Nexus 670) which was operated in He gas atmosphere (20 psi) at 25 °C with a purging gas time of 1 min. The true density of MWNT was measured repeatedly 20 times to obtain the average value and the standard deviation.

The electrical conductivity measurement (Keithley, Model 8009A) of the MWNT film samples was measured at 25 °C, the fixture consisted of two probes that made contact with the surface of the MWNT film samples. The test fixture was connected to the power source (Keithley, Model 6517A) to supply a constant voltage source and for reading the resultant current. The applied voltage and the resultant current were used to determine electrical conductivity of the MWNT film samples by the following Eq. (5.1):

$$\sigma = \frac{I}{\rho} = \frac{I}{R_s t} = \frac{I}{KVt} \tag{5.1}$$

where σ is the specific conductivity (S/cm), ρ is the specific resistivity (Ω cm), t is the specimen thickness (cm), R_s is the sheet resistivity (Ω), I isthe measured current (A), K is the geometric correction factor, and V is the applied voltage (V).

Scanning electron micrographs were taken with a scanning electron microscope (SEM; S-4800, Hitachi, Tokyo, Japan) to determine the morphology and sizes of the MWNT in a powder form, prestine gelatin, and MWNT/gelatin composites at various MWNT concentrations. The cross-section micrographs of gelatin and MWNT/gelatin composites were obtained by using an acceleration voltage of 10 kV with magnifications of 60 000 times. SEM imaging software (SEMAFORE 5.21) was used to provide tube diameter.

The topology and phase images of specimens were obtained from the atomic force microscopy (AFM, Park system, XE-100) where images were taken in the non–contact mode with the cantilever (NSC-14-CrAu) tapping at a scan rate of 0.25 Hz. The electrostatic force microscope (EFM) was determined at signal amplitude of 5 V, and a scan size of $1.25 \times 1.25\ \mu m^2$. Each sample was scanned at two height levels above the surface. In the first level, tip scanned the surface to obtain the topology images in the non–contact AFM mode in response to the Van der Waals forces. The second scan was carried out by measuring the tip-surface distance as a result of the electrostatic force. The charge distribution and the degree of charge generated were obtained from the EFM technique.

A melt rheometer (Rheometric Scientific, ARES) was used to study the electromechanical properties of the MWNT/Gelatin hydrogel composites. They were fitted with a custom-built copper parallel plate fixture of 30-mm diameter. A DC voltage was applied at the electric field strength of 800 V/mm using a DC power supply (Instek, GFG8216A). First, a strain sweep test was operated to determine the suitable strain for measuring storage modulus (G') in the linear viscoelastic regime. The appropriate strain was determined to be 0.10% for both pure gelatin hydrogel and the MWNT/Gelatin hydrogel composites. Prior to the temporal sweep and the frequency sweep test, samples were pre sheared at a low frequency (0.039811 rad/s) and low strain (0.10%) with the application of electric field (800 V/mm) for 15 min to ensure the formation of equilibrium polarization. In both experiments, the specimens were measured as functions of electric field strength (0–800 V/mm) and temperature (30–80 °C). The deflections of the pure gelatin hydrogel and the MWNT/Gelatin hydrogel composites were carried out under various applied electric strengths. For each hydrogel, one end of the sample was fixed vertically with a grip

between two parallel electrodes in a transparent chamber containing polydimethylsiloxane (PDMS, viscosity 100 cSt). The input electric field strength was provided by a DC power supply (Gold Sun 3000, GPS 3003D) connected to a high voltage power supply (Gamma High Voltage, UC5-30P), which can deliver various electric field strengths from 25 to 600 V/mm. A digital video recorder (Sony, Handicam HR1) was used to record the displacement of the composites. The bending distances of the composites were measured from a Scion Image (Beta 4.0.3) program.

The dielectrophores is force (F_d) on the samples was calculated through the static horizontal force balance consisting of the elastic force (F_e), the gravity force, and the buoyancy force as shown in Eq. (5.2)

$$F_d = F_e + mg(\sin\theta) - \rho Vg(\sin\theta) \tag{5.2}$$

where m is the mass of sample (kg), g is the gravity constant (9.8 m/s^2), θ is the deflection angle, ρ is the density of fluid, V is the volume of the displaced fluid, and F_e is the resisting elastic force (N). In our experiment, the elastic force can be calculated by the following Eq. (5.3) (Sato *et al.*, 1996; Timoshenko *et al.*, 1970):

$$F_e = \frac{dEI}{l^3} \tag{5.3}$$

where E is the young's modulus which is equal to $2G'(1+\nu)$ in which G' is the shear modulus (taken to be G' (ω = 1 rad/s)) and ν is the Poisson's ratio, which is equal to 1/2 for an incompressible sample, I is the moment of inertia $t^3w/12$, t is the thickness of specimen, w is the width of specimen, d is the deflection distance, and l is the length of specimen

5.4 Results and Discussion

5.4.1 Characterization of Multi-walled Carbon Nanotubes (MWNTs)

Characteristics of MWNTs are summarized in Table 5.1. True densities of four MWNTs are 2.143 ± 0.15, 2.140 ± 0.10, 2.170 ± 0.13, and 2.103 ± 0.10 g/cm^3, independent of different aspect ratio values. Our measured true density values are similar to the value (~2.1 g/cm^3) as reported by Lehman *et al.* (2011).

The average diameters of the tubes at various aspect ratios as measured by SEM are 9.47 ±1.59, 18.38 ± 0.43, 27.09 ± 0.10, and 42.63 ± 3.85 nm, which are consistent with the supplier material specification.

The specific conductivity values of MWNTs are approximately 3237, 2161, 1977, and 1693 S/cm (with standard deviations of 240, 328, 195, and 142 S/cm), respectively as shown in Table 5.1. Thus, the electrical conductivity of the lowest aspect ratio possesses the smallest value due to the presence of various defects formed with in MWNTs (Li *et al.*, 2007). A larger diameter MWNTs has a higher amount of defects (Du *et al.*, 2007). For typical single-walled carbon nanotubes, the specific electrical conductivity is of the order of 10^3 S/cm (Bandaru, 2007). Dai *et al.* (1996) reported that the electrical conductivity of MWNTs at ambient temperature is between 1250 and 8333 S/cm.

5.4.2 Morphology of Gelatin Hydrogel and MWNT/Gelatin Hydrogel Composites

Cross-sectioned scanning electron micrographs of the gelatin hydrogel and composites are shown in Fig. 5.1a–c at 0.1 and 1 vol% MWNT. It can be seen that the MWNT shows a moderate uniform dispersion in the gelatin hydrogel at low MWNT concentration (0.1 vol%) with the aid of the surfactant, owing to the attraction of hydrophobic chain of SDS molecule around the surface of MWNTs (Richard *et al.*, 2003). In Fig. 5.1c, the dispersion of MWNT at high concentration (1 vol%) is relatively poor because of the difficulty in obtaining homogeneous dispersion of 1 vol% MWNT in gelatin solution as due to the large van der Waals attraction forces between MWNT molecules.

The topology and the phase charged surface of the MWNT/Gelatin hydrogel composites were also investigated by the EFM phase measurement as shown in Fig. 5.2. The topology of the pure gelatin hydrogel and the 0.1 and 1 vol%

MWNT/Gelatin hydrogel composites without electrical charge are shown in Fig. 5.2a–c. Fig. 5.2a shows the smooth surface of the pure gelatin hydrogel at a nanoscale. A micrograph of the 0.1 vol% MWNT/gelatin hydrogel composite shows a well-distributed and randomly-aligned MWNT by the mechanical stirring force as shown in Fig. 5.2b. On the contrary, Fig. 5.2c demonstrates the agglomerated topology of 1 vol% MWNT/gelatin hydrogel composites. Fig. 5.2a′–c′ show the phase charged image of the pure gelatin hydrogel and the MWNT/gelatin hydrogel composites. The images exhibit the charge distributions within the materials where the light areas indicate the presence of the attractive charge generated between the probe tip and the materials. The degree of attractive charge generated on the pure gelatin hydrogel and the MWNT/Gelatin hydrogel composites is shown in Fig. 5.3. Both 0.1 and 1 vol% MWNT/gelatin hydrogel composites possess the degrees of attractive charge generated of 101 and 106% respectively, values which are greater than that of the pure gelatin hydrogel.

5.4.3 Electromechanical Properties

5.4.3.1 Time Dependence of Elctrorheological Response

The temporal response of the pure gelatin and the MWNT/gelatin hydrogel composites (0.1 vol% and 1 vol% MWNT) was investigated under the applied electric field strength of 800 V/mm as the electric field was switched on and off alternately. The temporal characteristics of materials were measured in the linear viscoelastic regime at a strain of 0.10%, and frequency of 100 rad/s. Fig. 5.4 shows the storage modulus (G') of the pure gelatin and of the MWNT/gelatin hydrogel composites during the time sweep tests under the electric field. For the pure gelatin hydrogel, when the electric field is switched on at 800 V/mm, G' immediately increases and rapidly reaches a steady-state value as the dipole moment within the materials are induced. As the electric field is switched off, G' decreases instantaneously close to its original value which can be referred to a reversible material. In contrast, for both MWNT/gelatin hydrogel composites (0.1 vol% and 1 vol% MWNT), G' decreases after switching off the electric field but it

does not recover to their original values. These characteristics indicate that there are some residue dipole moments due to the agglomerations of the MWNT.

5.4.3.2 *Effects of Electric Field Strength and Aspect Ratio on Electromechanical Properties of MWNT/Gelatin Hydrogel Composites*

Effect of MWNT aspect ratios (470, 740, 1200, and 2100) on the electromechanical properties of 0.1 vol% MWNT/gelatin hydrogel composites was first investigated in the range of 0 to 800 V/mm. Fig. 5.5 shows the storage modulus response ($\Delta G'$) and the storage modulus sensitivity ($\Delta G'/G'_o$) of the composites vs. electric field strength at a frequency of 100 rad/s, a strain of 0.10%, and at a temperature of 30 °C. It can be seen that $\Delta G'$ and $\Delta G'/G'_o$ of 0.1 vol% MWNT/gelatin hydrogel composites increase with increasing aspect ratio of MWNT and with increasing of electric field strength as the polarization is generated on carboxyl groups on the gelatin side chain . the dipole moment. leading to intermolecular interactions (Tungkavet *et al.*, 2012). The main reason is the higher response with increase of MWNT aspect ratio is be due to the stronger interfacial force between the nanotube and the matrix due to a higher surface area (Ayatollahi *et al.*, 2011), or the nanotube-matrix interaction.

Ayatollahi *et al.* (2011) reported the mechanical properties of epoxy/0.5 wt% MWNT at various aspect ratios (455, 555, 715, and 1000). Both of the modulus of elasticity and the tensile strength of the samples increased with increasing of aspect ratio. Manoharan *et al.* (2009) reported that MWNT with a smaller diameter enhanced a stronger interface with the polymer matrix due to the higher surface area of the nanotube. Boo *et al.* (2007) studied the effect of nanoplatelet structure on mechanical properties of epoxy nanocomposites. They found that the larger surface area increased the modulus of epoxy/ZrP-1000 relative to than that of epoxy/ZrP-100. A larger surface area is a result of a higher aspect ratio ZrP nanoplatelets induces an increase in the modulus.

5.4.3.3 *Effect of Concentration on Electromechanical Properties of MWNT/Gelatin Hydrogel Composites*

The effect of MWNT concentration on the electromechanical properties of MWNT/gelatin hydrogel composites was studied at 30 °C with the electric field strength varying between 0 and 800 V/mm. Fig. 5.6 shows the storage modulus response ($\Delta G'$, ω = 100 rad/s) of the gelatins at various MWNT contents of 0, 0.01, 0.1, 0.5 and 1 vol%. $\Delta G'$ increases nonlinearly with increasing electric field strength. With increasing MWNT concentration from 0 to 0.1 vol%, $\Delta G'$ increases from 82 507 to 223 600 Pa at an applied electric field strength of 800 V/mm. Further increase in the MWNT concentration (at 0.5 and 1 vol%) leads to a reduction of $\Delta G'$. Interestingly, $\Delta G'$ of the 1 vol% MWNT/gelatin hydrogel composite is inferior when compared to the pure gelatin hydrogel. Table 5.2 lists the storage modulus sensitivity ($\Delta G'/G'_o$) values of these materials at various MWNT contents. As MWNT concentration increases, the induced dipole moment increases under the applied electric field strength (Shiga, 1997) due to the enhanced polarizability of the carboxyl groups of gelatin chains under the presence of MWNT. The maximum $\Delta G'$ and $\Delta G'/G'_o$ are found in the 0.1 vol% MWNT/gelatin hydrogel composite. However, as the MWNT content is higher than 0.1 vol%, $\Delta G'$ decreases. As the highest MWNT concentration of 1 vol%, $\Delta G'$ under the applied electric field diminishes since the material presumably consists of the phase separation between the hydrogel and the MWNT agglomeration as previously observed in the SEM image and topology surface (see Fig. 5.1c and 5.2c).

Ayatollahi *et al.* (2011) found the similar behavior in that the Young's modulus and the tensile strength of epoxy/MWNT composites increased with increasing of MWNT. However at the higher MWNT concentration of 0.5 wt%, the mechanical properties decreased due to the effect of agglomeration. Prashantha *et al.* (2009) reported the optimum mechanical properties of multi walled carbon nanotube filled polypropylene nanocomposite, 2 wt% MWNT was the optimum concentration to enhance the modulus of the composite due to the dispersion and the distribution of individual nanotubes in the matrix. Evingur *et al.* (2012) studied the elasticity modulus of polyacrylamide (PAAm)/multi walled carbon nanotube (MWNT). The elastic modulus of PAAm/MWNT increased with increasing of MWNT concentration. However at the higher nanotube concentration of 5 wt%, the elastic modulus decreased. Kunanuruksapong *et al.* (2007) reported a similar effect

for poly(*p*-phenylene)/acrylic elastomer blended. The storage modulus response ($\Delta G'$) of poly(*p*-phenylene)/acrylic elastomer blended increased with increasing poly(*p*-phenylene) concentration. The maximum $\Delta G'$ occurred with 30 vol% poly(*p*-phenylene)/acrylic elastomer blended. For the highest particle concentration of 40 vol%, $\Delta G'$ diminished.

5.4.3.4 Effect of Operating Temperature

The electromechanical properties of the pure gelatin and the MWNT/gelatin hydrogel composites were investigated at the temperature range between 30 and 90 °C. The result shows that storage modulus at 800 V/mm (G') and storage modulus response ($\Delta G'$) of the composites exhibit three response regimes as shown in Fig. 5.7. With increasing temperature from 30 to 40 °C, G' of the pure gelatin hydrogel decreases because the triple-helix structure is split to the random coil structure (Bigi *et al.*, 2004). At the temperature range of 40–50 °C, G' increases again with temperature. According to the classical network theory (Sato *et al.*, 1996), as temperature increases, the entropy of gel increases that leading to more retractive force. However further increase in temperature (from 60 to 90 °C) leads to a decrease in G' since α-amino acid block of the gelatin chain is isolated at a temperature close to the low-temperature glass transition of 120 °C (Fraga *et al.*, 1985). Similar electromechanical properties are observed during the same temperature range for the 0.1 vol% MWNT/gelatin hydrogel composite, the level of triple-helix structure denaturation (30–40 °C) and the lower temperature glass transition temperature (~60–80 °C) of the composite could be retarded due to the enhanced polarizability of the carboxyl groups in the gelatin chains. The obtained result indicates that the electromechanical responses of the MWNT/gelatin hydrogel composites are largely improved in term of $\Delta G'$ due to the presence of MWNT. At any temperatures studied, $G'_{800v/mm}$ and $\Delta G'$ are higher than those of the pure gelatin hydrogel because MWNT acts as reinforced particles and enhances the polarizability in the gelatin chains under the electric field.

5.4.4 Deflection of MWNT/Gelatin Hydrogel Composites

The bending behavior and the dielectrophoresis force were investigated under the applied electric field strength between 0 and 600 V/mm. Samples were gripped between copper plates and immersed in a silicone oil chamber (shown in Fig. 5.8). The amount of deflection of the pure gelatin and MWNT/gelatin hydrogel composites at the specific electric field strength is described by the parameters (d, l, and θ). A video recorder (Sony, Handicam HR1) was used to record the displacement of the pure gelatin and MWNT/gelatin hydrogel composites. The bending behavior of the pure gelatin and all MWNT/gelatin hydrogel composites is shown in Fig. 5.9a–c. Results show that all of the samples bend toward the anode side (positive charge) under the influence of the electric field strength of 600 V/mm due to the attractive force between the polarized carbonyl group of hydrogel and the anode side. The polarization of the carbonyl groups can be referred to as the electrophilic behavior which generates the negative charges on their groups. As a higher electric field strength is applied, stronger dipole moments are generated leading to a higher degree of deflection. The pure gelatin, 0.1 vol% MWNT/gelatin, and 1 vol% MWNT/gelatin hydrogels start to deflect at lower critical electric field strengths of 100 V/mm, 100 V/mm, and 250 V/mm, respectively. The 0.1 vol% MWNT/gelatin hydrogel composite exhibits the greatest deflection values relative to other samples. The degree of deflection (θ) of 0.1 vol% MWNT/gelatin hydrogel composite is higher than the pure gelatin hydrogel due to the higher amount of polarizability from MWNT. In contrast, the 1 vol% MWNT/gelatin hydrogel composite shows a lesser deflection response than the other two samples due to too high particle contents (Krause and Bohon, 2001). The induction times of these samples of deflection response are tabulated in Table 5.3. The induction time is the time which is required for the sample to deflect toward the maximum distance in the influence of applied electric field strength. All of the samples studied exhibit fast deflection response which is one of the importance factors for actuator application. Fig. 5.10 a–b shows the deflection distances and the dielectrophoresis forces (F_d) of the pure gelatin and the MWNT/gelatin hydrogel composites under electric field strength. The deflection distances and the dielectrophoresis forces of these materials become larger with increasing electric field strength. At electric field strength of 600

V/mm, F_d of the pure gelatin hydrogel, 0.1 vol% MWNT/gelatin, and 1.0 vol% MWNT/gelatin hydrogel composites are 0.036, 0.039, and 0.031 N, respectively. The F_d of 0.1 vol% MWNT/gelatin hydrogel composites is the highest since such a composite has a higher amount of polarized nanotube content that creates a stronger attractive with the anode side. However, the 1 vol% MWNT/gelatin hydrogel composite shows a lower F_d than the pure gelatin and 0.1 vol% MWNT/gelatin hydrogel composite due to the particle steric hindrance (Liu and Shaw, 2001).

In the previous works, Niamlang *et al.* (2008) investigated dielectrophoresis force and deflection of poly(p-phenylenevinylene)/polydimethylsiloxane blends (PPV/PDMS). The dielectrophoresis force and the degree of deflection of the PPV/PDMS films increased with increasing electric field strength. The maximum dielectrophoresis force was found in PPV/PDMS-10 because of a higher amount of polarized particles; however, the PPV/PDMS-20 showed a lower dielectrophoresis force than PPV/PDMS-10 due to the too high particle concentration and the particle steric hindrance. Kunchornsup *et al.* (2012) reported the dielectrophoresis force of cellulose gel under the electric field strength between 0 and 550 V/mm. At 500 V/mm, the cellulose gel showed the dielectrophoresis force of 4.6 N and deflection angle at 44°, respectively. In addition, with increasing electric field strength between 525 and 550 V/mm, the back and forth swinging deflection occurred due to the competition between the anion and cation movements in the ionic liquid. Tungkavet *et al.* (2012) reported the dielectrophoresis forces at E = 600 V/mm of 0.1 vol% and 1 vol% nanowire-Ppy gelatin hydrogels to be 6.60 and 1.60 mN, respectively since the 1 vol% nanowire-Ppy has strong positive charges that counteract those of negative charges in gelatin structure and the effect of steric hindrance. Petcharoen *et al.* (2013) studied the dielectrophoresis force of thermoplastic polyurethane elastomer (TPE-PU). TPE-PU generated the highest dielectrophoresis force (43 μN) and deflection distance (10 mm) at electric field strength of 500 V/mm. In this work, 0.1 vol% MWNT/gelatin hydrogel composite provide the greatest deflection distance at 14.50 mm and the maximum dielectrophoresis force of 0.039 N.

5.5 Conclusions

This work presents the electromechanical properties, the dymanic storage moduli (G') and the bending measurement of pure gelatin and MWNT/gelatin hydrogel composites as functions of electric field strength and temperature. When the electric field is applied, the polarization generated in gelatin chain is further enhanced by the presence of MWNT, as induced by electrostatic interaction. Both of the storage modulus response ($\Delta G'$) and the storage modulus sensitivity ($\Delta G'/G_o$) increase with increasing electric field strength upto 800 V/mm. The maximum $\Delta G'$ and $\Delta G'/G_o$ are 2.34×10^5 Pa and 1.25, respectively, for the 0.1 vol% MWNT/gelatin hydrogel composite. For the effect of temperature, both G' and $\Delta G'$ exhibit three behaviors between 30 and 90 °C. From the deflection measurement, the deflection distance and the dielectrophoresis force (F_d) of the pure gelatin and 0.1 vol% and 1 vol% MWNT/gelatin hydrogel composites increase with increasing electric field strength. The 0.1 vol% MWNT/gelatin hydrogel composite exhibits the greatest deflection response; whereas the 1 vol% MWNT/gelatin hydrogel composite shows the lowest deflection distance and F_d due to the particle steric hindrance.

5.6 Acknowledgements

The authors would like to acknowledge the financial supportsfrom the Conductive and Electroactive Polymers Research Unit of Chulalongkorn University; the Thailand Research Fund (TRF); the Royal Thai Government; the 90th Anniversary of Chulalongkorn University Fund (Ratchadaphiseksomphot Endowment Fund); the Petroleum and Petrochemical College (PPC), Chulalongkorn University; and the Doctoral Scholarship from the Thailand Graduate Institute of Science and Technology (TGIST) (TG-33-09-53-003D).

5.7 References

Ayatollahi, M.R., Shadlou, S., Shokrieh, M.M., and Chitsazzadeh, M. (2011) Effect of multi-walled carbon nanotube aspect ratio on mechanical and electrical properties of epoxy-based nanocomposites. Polymer Testing, 30, 548–556.

Bandaru, P.R. (2007) Electrical properties and applications of carbon nanotube structures. Journal of Nanoscience and Nanotechnology, 7, 1–29.

Bigi, A., Panzavolta, S., and Rubini, K. (2004) Relationship between triple-helix content and mechanical properties of gelatin films. Biomaterials, 25, 5675-5680.

Boo, W.J., Sun, L., Warren, G.L., Moghbelli, E., Pham, H., Clearfield, A., and Sue, H.J. (2007) Effect of nanoplatelet aspect ratio on mechanical properties of epoxy nanocomposites. Polymer, 48, 1075–1082.

Bower, C., Rosen, R., and Jin, L. (1999) Deformation of carbon nanotubes in nanotube-polymer composites. Applied Physics Letters, 74, 3317–3319.

Dai, H., Wong, W., and Lieber, C.M. (1996) Probing electrical transport in nanomaterials: Conductivity of individual carbon nanotubes. Science, 272, 523–526.

Du, C. and Pan, N. (2007) Carbon nanotube-based supercapacitors. Nanotechnology Law & Business, 4, 569–576.

Evingur, G.A. and Pekcan, O. (2012) Temperature effect on elasticity of swollen composite formed from polyacrylamide (PAAm)-multiwall carbon nanotubes (MWNTs). Engineering, 4, 619–624.

Fraga, A.N. and Williams, R.J.J. (1985) Thermal properties of gelatin films. Polymer, 26, 113-118.

Guo, Z., Sadler, P.J., and Tsang, S.C. (1998) Immobilization and visualization of DNA and protein on carbon naotubes. Advanced Materials, 10, 701–703.

Haider, S., Park, S.Y., Saeed, K., and Farmer, B.L. (2007) Swelling and electroresponsive characteristics of gelatin immobilized onto multi-walled carbon nanotubes. Sensor and Actuators B: Chemical, 124, 517-528.

Kaewpirom, S. and Boonsang, S. (2006) Electrical response characterization of poly(ethylene glycol) macromer (PEGM)/chitosan hydrogels in NaCl solution. European Polymer Journal, 42, 1609–1616.

Kim, S.J., Lee, K.J., Kim, S.I., Lee, Y.M., Chung, T.D., and Lee, S.H. (2002) Electrochemical behavior of an interpenetrating polymer network hydrogel composed of poly(propylene glycol) and poly(acrylic acid). Journal of Applied Polymer Science, 89, 2301–2305.

Kim, S.J., Park, S.J., Kim, I.Y., Shin, M.S., and Kim, S.I. (2002) Electric stimuli response to poly(vinyl alcohol)/chitosan interpenetrating polymer network hydrogel in NaCl solutions. Journal of Applied Polymer Science, 86, 2285–2289.

Kim, S.Y., Shin, H.S., Lee, Y.M., and Jeong, C.N. (1999) Properties of electroresponsive poly(vinyl alcohol)/poly(acrylic acid) IPN hydogels under an electric stimulus. Journal of Applied Polymer Science, 73, 1675–1683.

Krause, S. and Bohon, K. (2001) Electromechanical response of electrorheological fluids and poly(dimethylsiloxane) networks. Macromolecule, 34, 7179–89.

Kunanuruksapong, R. and Sirivat, A. (2007) Poly(p-phenylene) and acrylic elastomer blends for electroactive application. Material Science and Engineering: A, 454-455, 453-460.

Kunchornsup, W. and Sirivat, A. (2012) Physically cross-linked cellulosic gel via 1-butyl-3-methylimidazolium chloride ionic liquid and its electromechanical responses, Sensors and Actuators A: Physical, 175, 155–164.

Lehman, J.H., Terrones, M., Mansfield, E., Hurst, K.E., and Meunier, V. (2011) Evaluating the characteristics of multiwall carbon nanotubes. Carbon, 49, 2581–2602.

Li, H., Wang, D.Q., Chen, H.L., Liu, B.L., and Gao, L.Z. (2003) A novel gelatin-carbon nanotubes hybrid hydrogel. Macromolecule Bioscience, 3, 720–724.

Li, Q., Li, Y., Zhang, X., Chikkannanavar, S.B., Zhao, Y., Dangelewicz, A.M., Zheng, L., Doorn, S.K., Jia, Q., Peterson, D.E., Arendt, P.N., Zhu, Y. (2007) Structure-dependent electrical properties of carbon nanotube fibers. Advanced Materials, 19, 3358–3363.

Liu, B. and Shaw, T.M. (2001) Electrorheology of filled silicone elastomers. Journal of Rheology, 45, 641-657.

Macdonald, R.A., Laurenzi, B.F., Viswanathan, G., Ajayan, P.M., and Steqemann, J.P. (2005) Collagen-carbon nanotube composite materials as scaffolds in tissue engineering. Journal of Biomedical Material Research A, 74, 489–96.

Manoharan, M.P., Sharma, A., Desai, A.V., Haque, M.A., Bakis, C.E., and Wang, K.W. (2009) The interfacial strength of carbon nanofiber epoxy composite using single fiber pullout experiments. Nanotechnology, 20, 1–5.

Nguyen, T.H. and Lee, B.T. (2010) Fabrication and characterization of cross-linked gelatin electro-spun nano-fibers. Journal of Biomedical Science and Engineering, 3, 1117–1124.

Niamlang, S. and Sirivat, A. (2008) Dielectrophoresis force and deflection of electroactive poly(p-phenylene vinylene)/polydimethylsiloxane blends. Smart Materials and Structure, 17. 1–8.

Okano, T., Bae, Y.H., Jacobs, H., and Kim, S.W. (1990) Thermally on-off switching polymers for drug permeation and release. Journal of Control Release, 11, 255-265.

Park, T.G. and Hoffman, A.S. (1992) Synthesis and characterization of pH-and/or temperature-sensitive hydrogels. Journal of Applied Polymer Science, 46, 659–671.

Petcharoen, K. and Sirivat, A. (2013) Electrostrictive properties of thermalplastic polyurethane elastomer: Effects of urethane type and soft–hard segment composition. Current Applied Physics, 13, 1119–1127.

Prashantha, K., Soulestin, J., Lacrampe, M.F., Krawczak, P.G., Dupin, G., Claes, M. (2009) Masterbatch-based multi-walled carbon nanotube filled polypropylene nanocomposites: Assessment of rheological and mechanical properties. Composite Science and Technology, 69, 1756–1763.

Qian, D. and Dickey, E.C. (2000) Load transfer and deformation mechanisms in carbon nanotube-polystylene composites. Applied Physics Letters, 76, 2868–2870.

Richard, C., Balavoine, F., Schultz, P., Ebbesen, T.W., and Mioskowski, C. (2003) Supramolecular self-assembly of lipid derivatives on carbon nanotubes. Science, 300, 775–778.

Ross-Murphy, S.B. (1992) Structure and rheology of gelatin gels: Recent progress. Polymer, 33, 2622–2627.

Sato, T., Watanabe, H., and Osaki, K. (1996) Rheological and dielectric behavior of a styrene-isoprene-styrene triblock copolymer in n-tetradecane. 1. Rubbery-Plastic-Viscous transition. Macromolecule, 29, 6231-6239.

Shadler, L.S., Giannaris, S.C., and Ajayan, P.M. (1998) Load transfer in carbon nanotube epoxy composites. Applied Physics Letters, 73, 3842–3844.

Shiga, T. (1997) Deformation and Viscoelastic Behavior of Polymer Gels in Electric fields. Advances in Polymer Science. Berlin: Springer-Verlag.

Timoshenko, S.P. and Goodier, J.N. (1970) Theory of Elasticity. Auckland: McGraw-Hill.

Tungkavet, T., Pattavarakorn, D., and Sirivat, A. (2012) Bio-compatible gelatins (Ala-Gly-Pro-Arg-Gly-Glu-4Hyp-Gly-Pro-) and electromechanical properties: effects of temperature and electric field. Journal of Polymer Research, 19, 9759–3.

Tungkavet, T., Seetapan, N., Pattavarakorn, D., and Sirivat, A. (2012) Improvements of electromechanical properties of gelatin hydrogels by blending with nanowire polypyrrole: Effects of electric field and temperature. Polymer International, 61, 825–833.

Wagner, H.D., Lourie, O., Feldman, Y., and Tenne, R. (1998) Stress-induced fragmentation of multiwall carbon nanotubes in a polymer matrix. Applied Physics Letters, 72, 188–190.

Yang, X.J., Zheng, P.J., Cui, Z.D., Zhao, N.Q., Wang, Y.F., and Yao, K.D. (1997) Swelling behavior of elastic properties of gelatin gels. Polymer International, 44, 448–452.

Zareie, H.M., Bulmus, E.V., Gunning, A.P., Hoffman, A.S., Piskin, E., and Morris, V.J. (2000) Investigation of stimuli-responsive copolymer by atomic force microscopy. Polymer, 41, 6723–6727.

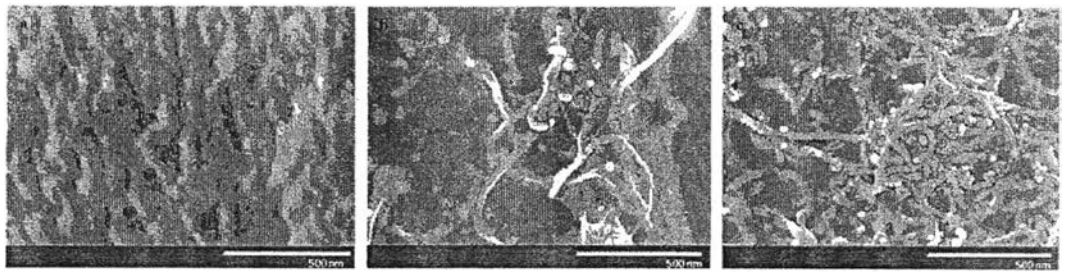

Figure 5.1 SEM micrograph of cross-sections of the pure gelatin and MWNT/gelatin hydrogels (magnification of 60K): (a) cross-sections of the pure gelatin; (b) cross-section of the 0.1 vol% MWNT/gelatin hydrogel; and (c) cross-section of the 1 vol% MWNT/gelatin hydrogel.

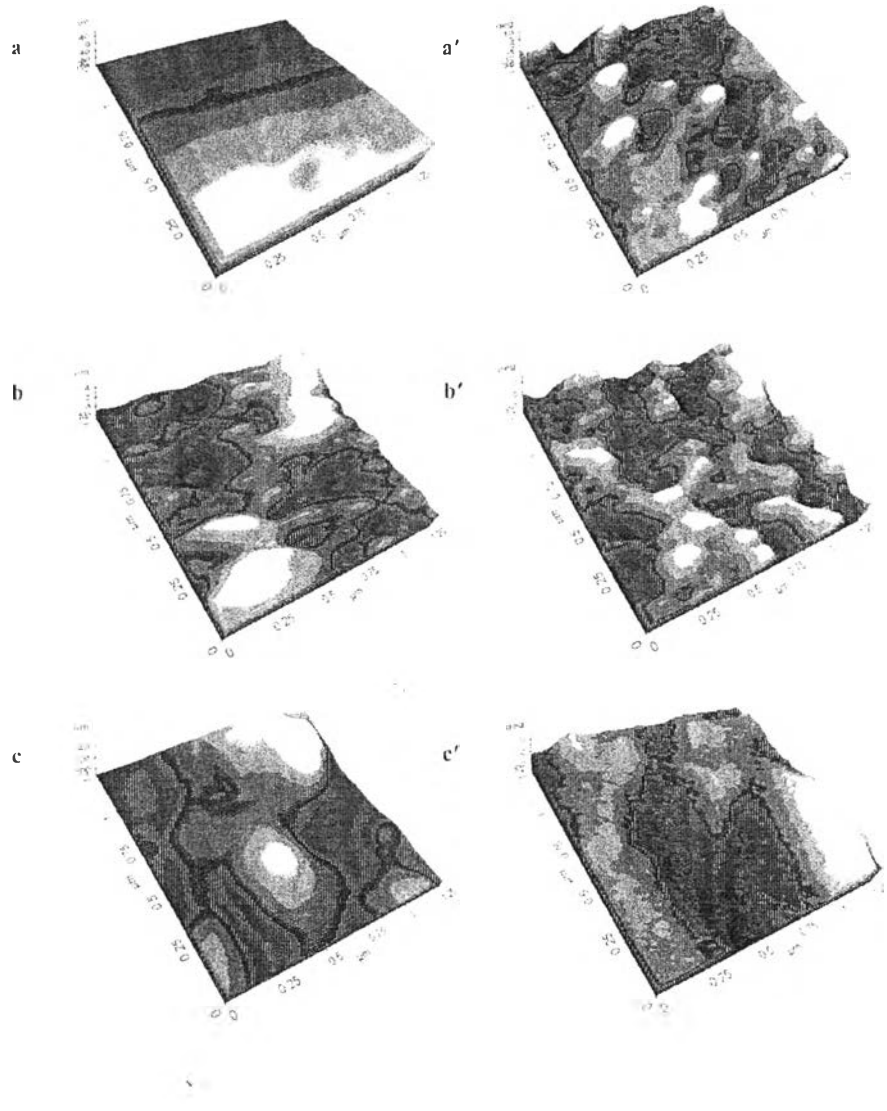

Figure 5.2 (a) Topology image of pure gelatin hydrogel; (a′) EFM image under 5 V of sample voltage bias of pure gelatin hydrogel; (b) Topology image of 0.1 vol% MWNT/gelatin hydrogel; (b′) EFM image under 5 V of tip voltage bias of 0.1 vol% MWNT/gelatin hydrogel; (c) Topology image of 1 vol% MWNT/gelatin hydrogel; (c′) EFM image under 5 V of tip voltage bias of 1 vol% MWNT/gelatin hydrogel.

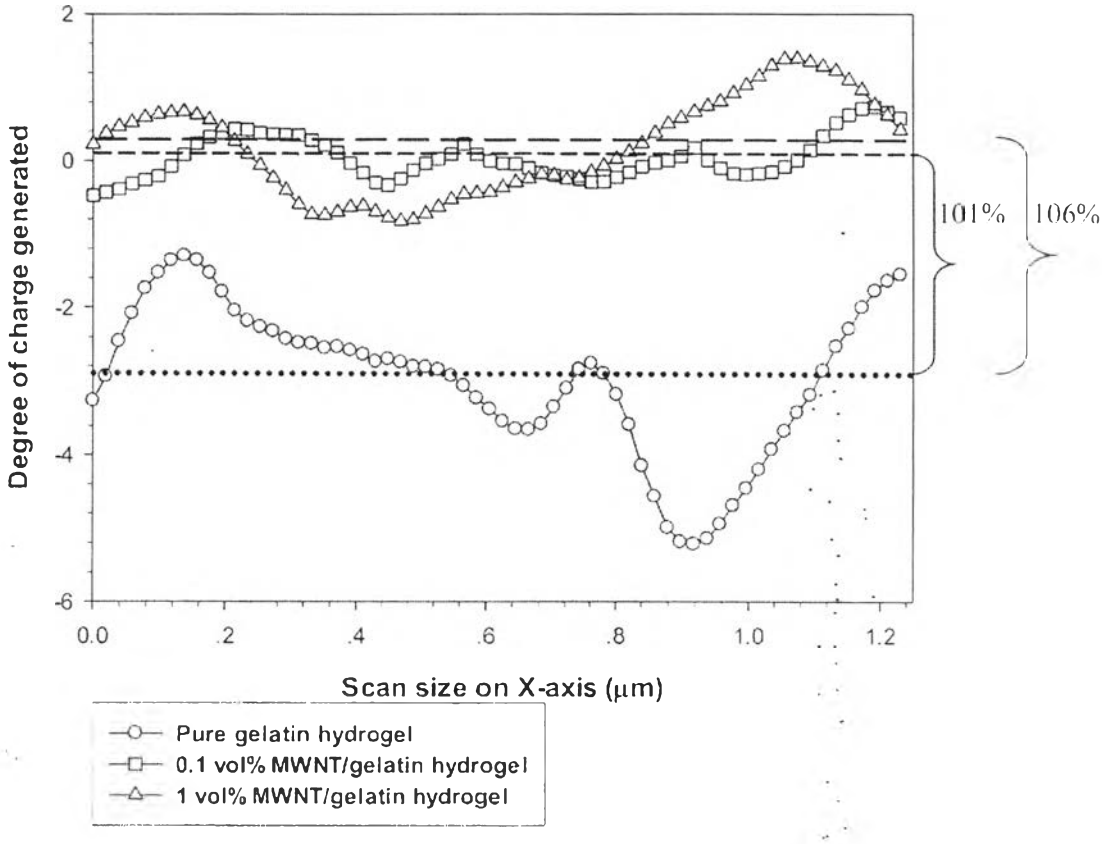

Figure 5.3 Degree of charge generated on MWNT/gelatin hydrogel under 5 V of tip bias at whole region.

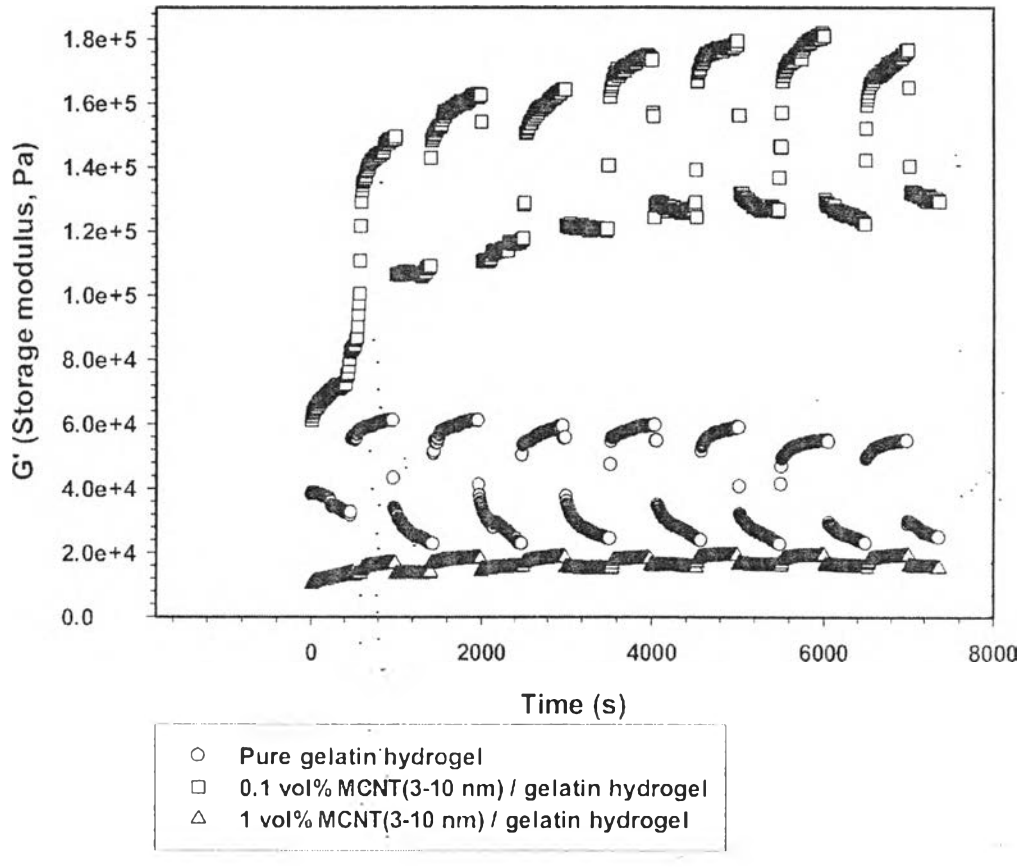

Figure 5.4 Temporal responses of the storage modulus (G′) of the pure gelatin hydrogel and the MWNT/gelatin hydrogels (sample diameter 30 mm, gel thickness 1.540 mm, 0.10 %strain, frequency of 100 rad/s, 800 V/mm, 30 °C): pure gelatin hydrogel (○); 0.1 vol% MWNT/gelatin hydrogel (□); 1 vol% MWNT/gelatin hydrogel (Δ).

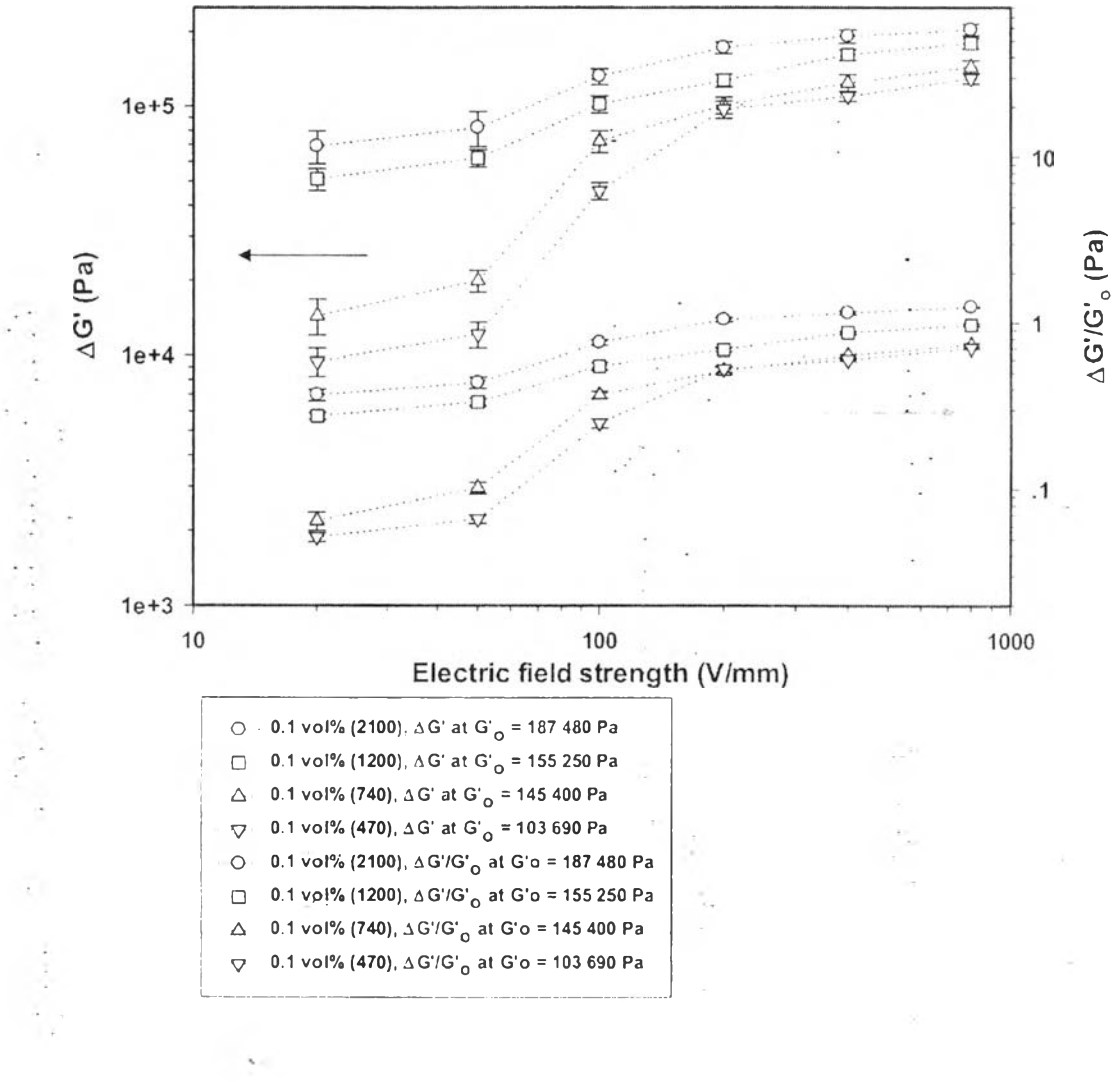

Figure 5.5 Effect of aspect ratios of MWNT on the storage modulus response ($\Delta G'$) and storage modulus sensitivity ($\Delta G'/G'_o$) at various electric field strengths (sample diameter 30 mm, gel thickness 1.640 mm, 0.10 %strain, frequency of 100 rad/s, 30 °C).

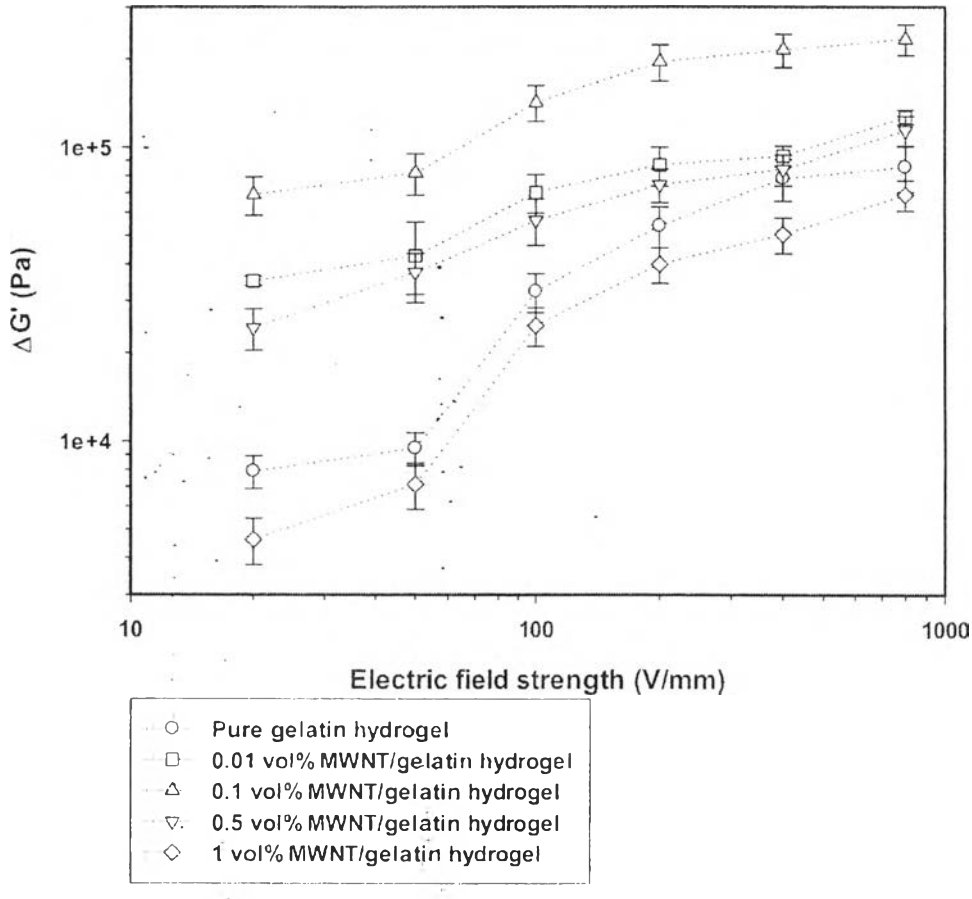

Figure 5.6 Effect of concentration of MWNT (2100) on the storage modulus response ($\Delta G'$) at various electric field strengths (sample diameter 30 mm, gel thickness 1.640 mm, 0.10 %strain, frequency of 100 rad/s, 30 °C).

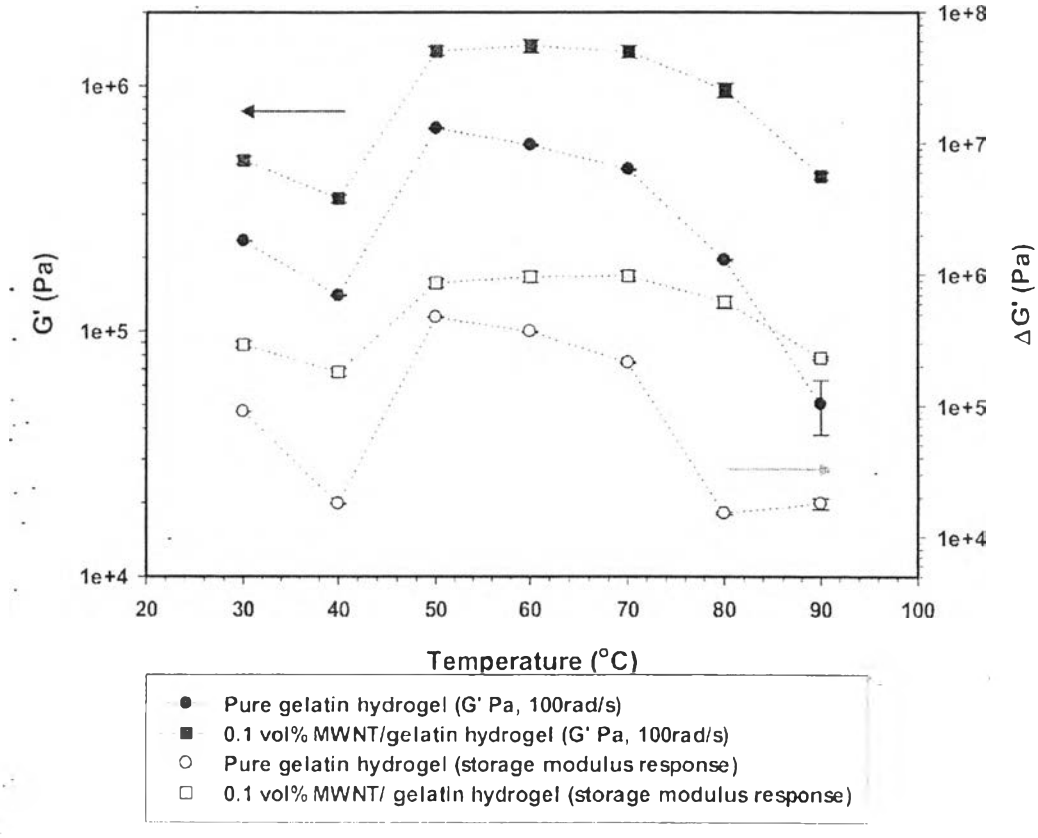

Figure 5.7 Effect of concentration of MWNT (2100) on the storage modulus (G') and storage modulus response ($\Delta G'$) at various temperature (sample diameter 30 mm, gel thickness 1.640 mm, 0.10 %strain, frequency of 100 rad/s, 800 V/mm).

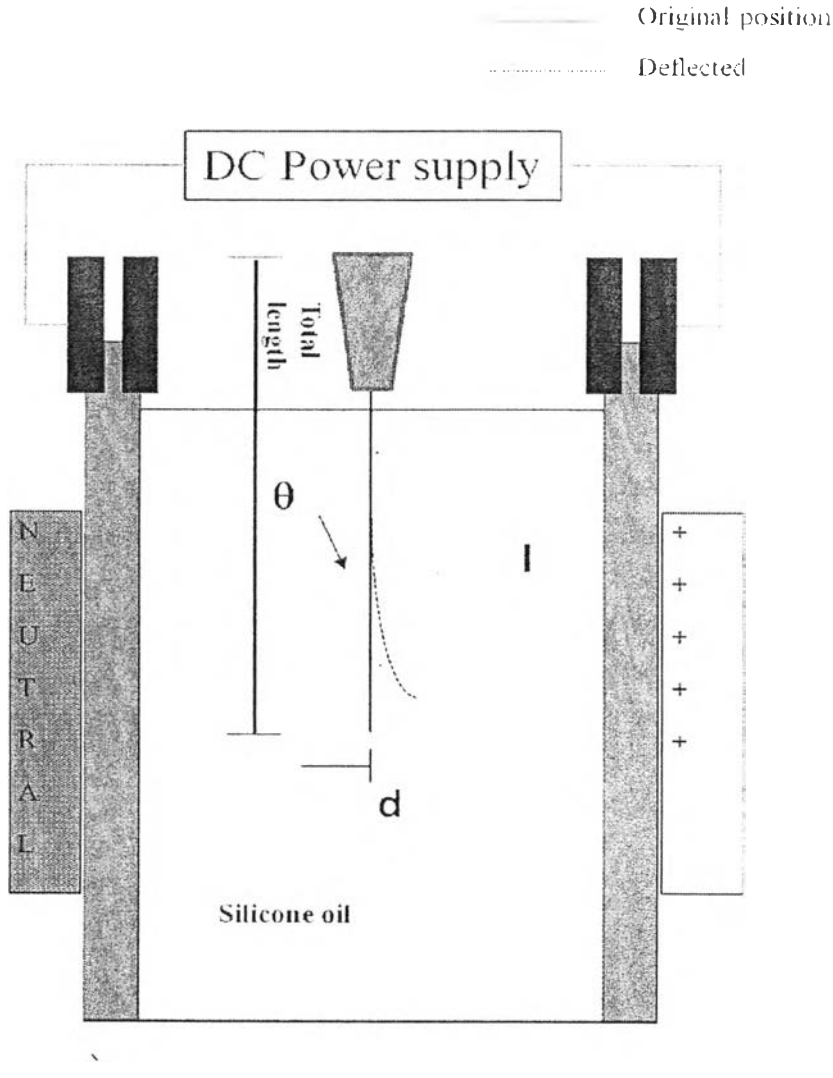

Figure 5.8 Schematic diagram of the apparatus used to observe the dielectrophoretics force on the hydrogel samples.

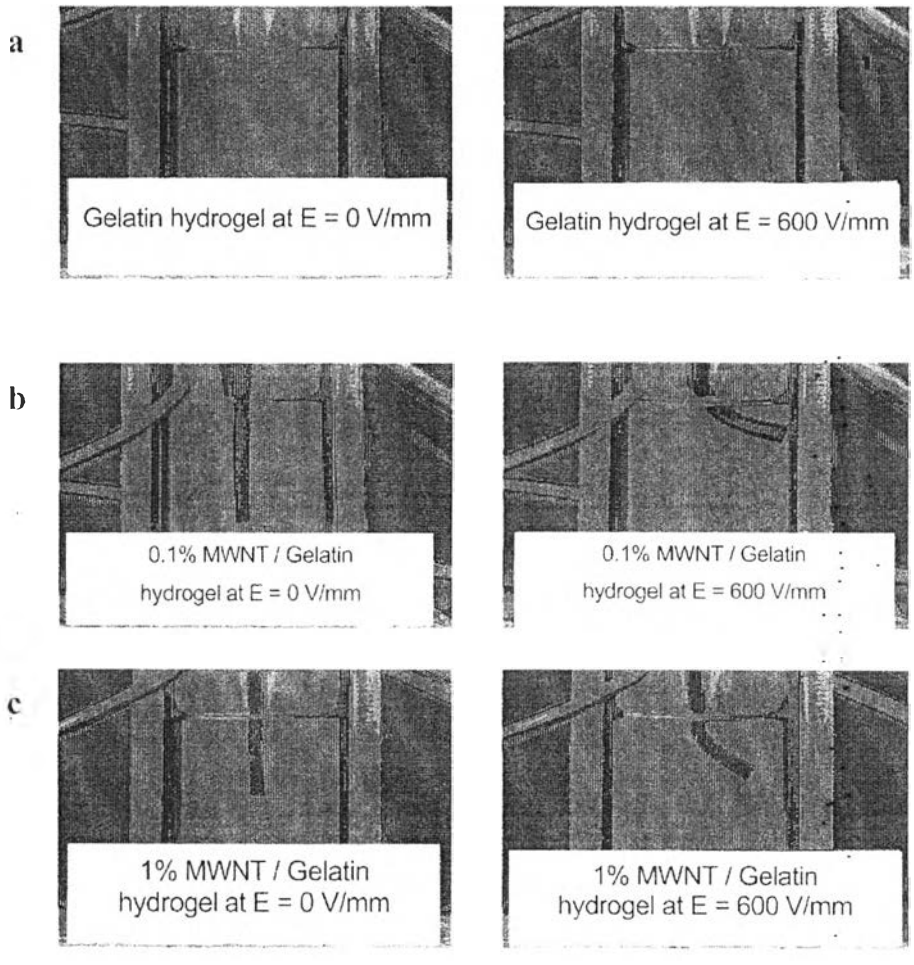

Figure 5.9 Deflection of the gelatin hydrogels at E = 0 and 600 V/mm : (a) pure gelatin hydrogel; (b) 0.1 vol% MWNT/gelatin hydrogel; (c) 1 vol% MWNT/gelatin hydrogel. (Note that the polarity of the electrode on the right-hand side is positive.)

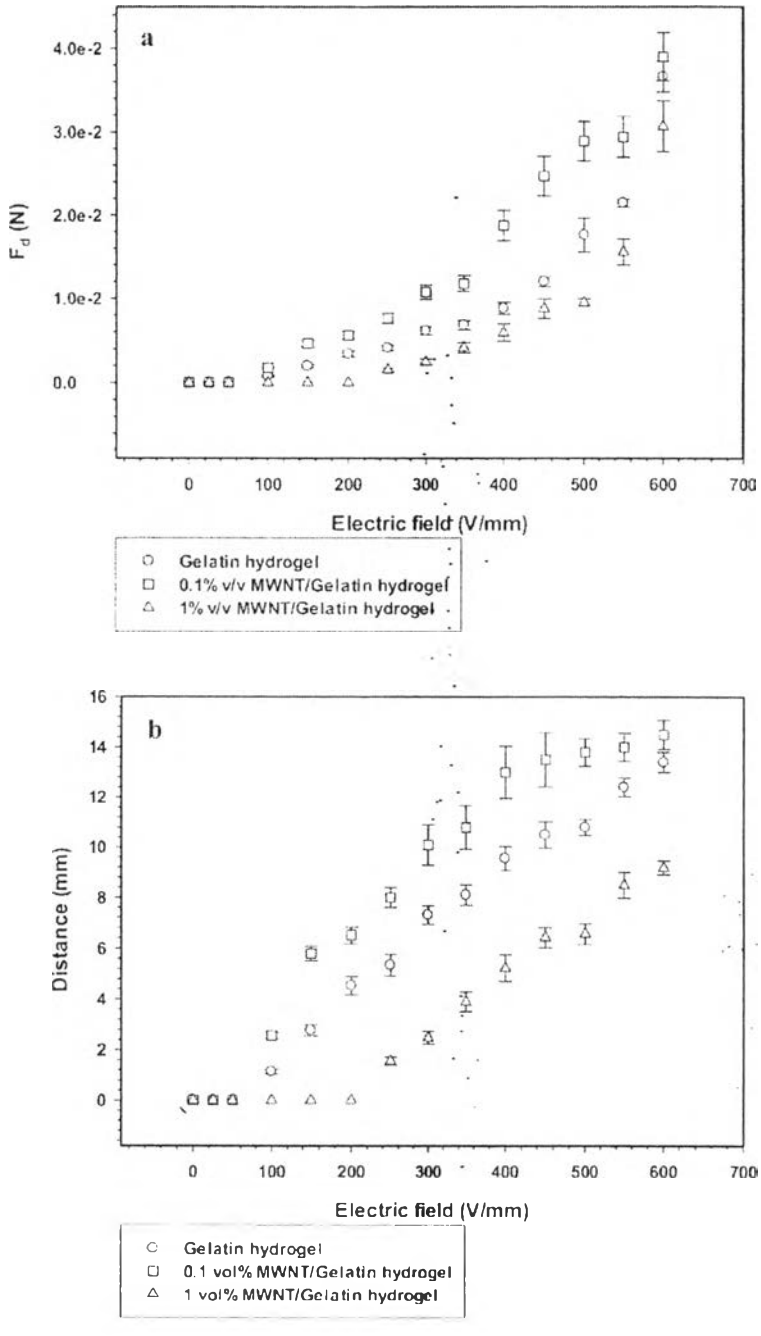

Figure 5.10 (a) Deflection distance of the pure gelatin hydrogel, the 0.1 vol% MWNT/Gelatin hydrogel, and the 1 vol% MWNT/Gelatin hydrogel at various electric field strengths. (b) Dielectropholetic force calculated through linear deflection theory.

Table 5.1 Determination of density, diameter, and conductivity of Multi-walled Carbon Nanotubes (MWNTs)

Samples	Quoted diameter of tube (nm)	Measured diameter of tubed	Aspect ratios	Density (g/cm^3)	Average conductivity (S/cm)
MWNTs	3-10	9.47 ± 1.59	2100	2.103 ± 0.10	3237 ± 240
	10-20	18.38 ± 0.43	1200	2.170 ± 0.13	2161 ± 328
	20-30	27.09 ± 2.39	740	2.140 ± 0.10	1977 ± 195
	30-50	42.63 ± 3.85	470	2.143 ± 0.15	1693 ± 142

Table 5.2 Sensitivity of storage modulus of the pure gelatin hydrogel and the MWNT (2100)/gelatin hydrogels (0.10% strain, electric field strength 800 V/mm, frequency 100 rad/s, 30 °C)

Materials (MWNT diameter 3-10 nm)	Storage modulus (G') (Pa)	Initial storage modulus (G_o') (Pa)	Sensitivity of storage modulus ($\Delta G'/G_o'$)
Pure gelatin hydrogel	2.60×10^5	1.78×10^5	0.47
0.01 vol% MWNT(2100)/gelatin hydrogel	3.08×10^5	1.81×10^5	0.70
0.1 vol% MWNT(2100)/gelatin hydrogel	4.21×10^5	1.87×10^5	1.25
0.5 vol% MWNT(2100)/gelatin hydrogel	2.34×10^5	1.20×10^5	0.94
1 vol% MWNT(2100)/gelatin hydrogel	1.53×10^5	8.50×10^4	0.81

Table 5.3 Induction time of MWNT/Gelatin hydrogel at various electric field strengths from deflection measurement: (a) pure gelatin hydrogel; (b) 0.1 vol% MWNT/Gelatin hydrogel; (c) 1 vol% MWNT/Gelatin hydrogel

Materials	**Induction time (s) at various electric field strength (V/mm)**							
	25	50	100	200	300	400	500	600
Pure gelatin hydrogels	-	-	10	8	7	7	6	4
0.1 vol% MWNT(3-10 nm)/gelatin hydrogel	-	-	6	6	4	3	2	1
1 vol% MWNT(3-10 nm)/gelatin hydrogel	-	-	7	6	6	4	3	2